

Supporting Information

Formation of Prenucleation Clusters and Transformation to ZnSe Quantum Dots and Magic-Size Clusters

Wenting Wang,¹ Qiu Shen,² Yusha Yang,²
Andrei Sapelkin,³ Shasha Wang,^{*,2} Chaoran Luan,^{*,4} Kui Yu^{1,2}

¹Institute of Atomic and Molecular Physics, Sichuan University,
Chengdu, 610065 Sichuan, P. R. China

²Engineering Research Center in Biomaterials, Sichuan University,
Chengdu, Sichuan, 610065, P. R. China

³Department of Physics and Astronomy, Queen Mary University of London
Mile End Road, London, E1 4NS, United Kingdom

⁴College of Biomedical Engineering, Sichuan University,
Chengdu, Sichuan, 610065, P. R. China

* Correspondence and requests for materials should be addressed to
S. W. (email: wangshasha502@163.com) or to C. L. (email: luanc@scu.edu.cn)

Table of Contents

Experimental Section		S3
Scheme S1	Generalization of the formation pathways for solids from solutions	S7
Table S1	Summary of hot-injection approaches to MSCs or QDs	S9
Table S2	Summary of heating-up approaches to MSCs or QDs	S11
Figure S1-1	Spectra of samples within 120 or 60 min from Fig. 1 reactions	S13
Figure S2-1	Spectra of 80 to 240 °C samples from Fig. 2 reactions	S14
Figure S2-2	MALDI-TOF MS of ZnSe PC-299 and MSC-299	S15
Figure S2-3	TEM of PC-299 and MSC-299	S16
Figure S3-1	Spectra of samples from the reactions of Fig. 3	S17
Figure S3-2	Spectra of Fig. 3 samples in CH	S18
Figure S3-3	Relation between the sample amount and the absorbance of MSC-299	S19
Figure S3-4	Spectra of 80 to 240 °C samples from heating-up reactions	S20
Figure S3-5	Spectra of samples from 120 °C reaction with [Se] = 45 mmol/kg	S21
Figure S3-6	Spectra of samples from 160 °C reaction with [Se] = 15 mmol/kg	S22
Figure S3-7	Spectra of 80 to 240 °C samples from reaction with [Se] = 15 mmol/kg	S23
Figure S4-1	Spectra of samples from Fig. 4 reactions with 2/5/6Zn to 1Se	S24
Figure S4-2	Spectra of samples from Fig. 4 reactions with 0.5/1/8Zn to 1Se	S25
Figure S4-3	Spectra of 80 to 240 °C samples from reaction with additional OA	S26
Figure S4-4	Spectra of samples from 120 °C reaction of 6Zn(OA) ₂ -1SeTOP-1DPP	S27
Figure S4-5	Spectra of samples from 200 °C reaction of 2Zn(OA) ₂ -1SeTOP-1DPP	S28
Figure S5-1	Spectra of Fig. 5 samples in CH	S29
Figure S5-2	Spectra of samples from reactions of 4Zn(OA) ₂ -1SeTOP-0.75DPP	S30
Figure S5-3	Comparison of OD value of samples from Figs. S2-1b and 5c	S31
Figure S5-4	Spectra of 80 to 240 °C samples from reaction with additional TOP	S32
Figure S6-1	Transformation of unpurified MSC-299	S33
Figure S6-2	Reversible transformation between MSC-299 and MSC-320	S34
Figure S6-3	Reversible transformation between MSC-299 and MSC-340	S35

Experimental Section

Materials. Tri-*n*-octylphosphine (TOP, 90.0%), oleic acid (OA, 90%), 1-octadecene (ODE, 90.0%), octylamine (OTA, 99.0%) and oleylamine (OLA, 70%) were obtained from Sigma-Aldrich. Zinc oxide (ZnO, 99.0%), methyl alcohol (MeOH, 99.5%), toluene (Tol, 99.5%) and cyclohexane (CH, 99.5%) were obtained from Chengdu Kelong Chemical. Acetonitrile (MeCN) was obtained from Tianjin Zhi Yuan Chemical. Selenium powder (Se, 99.99%) was obtained from Alfa-Aesar, and diphenylphosphine (HPPH₂/DPP, 98.0%) was obtained from J&K.

Zn(OA)₂ Stock Solution Preparation. ZnO (0.495 g, 6.04 mmol), OA (3.776 g, 13.20 mmol), and ODE (5.028 g) were mixed and added to a 50 mL three-necked flask under stirring at room temperature. The resulting mixture was evacuated for about 8 min, followed by purging with N₂ for 2 min. The evacuation-purging operation was repeated three times. The mixture was heated to 120 °C under a N₂ atmosphere and kept at this temperature for 2 hours. Then, the mixture was further heated to 290 °C, kept at 290 °C for 2 h to result in a transparent solution. The resulting solution was then cooled to 120 °C, followed by evacuating for 2 hours. The stock solution was stored under ambient conditions for further usage.

SeTOP Stock Solution Preparation. Se powder (0.328 g, 4.15 mmol), TOP (3.390 g, 9.15 mmol), and ODE (0.437 g) were loaded in a 25 mL three-necked flask at room temperature. Under a N₂ atmosphere, the mixture was stirred at room temperature to achieve a clear solution. The stock solution was stored in a glovebox for further usage.

Synthesis of ZnSe MSCs and QDs via Hot-Injection Approach. Zn(OA)₂ stock solution (1.842 g, 1.2 mmol) and ODE (2.875 g) were mixed and added to a 50 mL three-necked flask at room temperature. The mixture was heated to 80 °C, and then evacuated for 8 min and filled with N₂ for 2 min. This procedure was repeated three times until no bubbles were observed under vacuum. Under a N₂ atmosphere, the mixture was then heated to 120 °C, and kept at this temperature for 2 hours. Next, the mixture was heated to 240 °C or 260 °C (Figs. 1 and S1-1) under a N₂ atmosphere. The room-temperature mixture of SeTOP (330 μL, 0.30 mmol) and DPP (52 μL, 0.30 mmol) was swiftly added. The temperature dropped to 226

°C or 245 °C, and then was increased and kept at 230 °C or 250 °C. The total weight was 5.017 g with a Se concentration of 60 mmol/kg.

Synthesis of ZnSe MSCs and QDs via Heating-up Approach. Zn(OA)₂ stock solution (1.850 g, 1.2 mmol) and ODE (2.881 g) were mixed and added to a 50 mL three-necked flask at room temperature (Figs. 2 and S2-1). After heating the mixture to 80 °C under a N₂ atmosphere, the mixture was evacuated for about 8 min and purged with N₂ for 2 min; this procedure was repeated three times. Subsequently, the mixture was heated to 120 °C and evacuated for 2 h until no bubble appeared. Under a N₂ atmosphere, the resulting mixture was cooled to 80 °C which was a transparent yellowish solution. The SeTOP stock solution (0.307 g, 0.30 mmol), and DPP (52 μL, 0.30 mmol) were mixed in the glove box. Under a N₂ atmosphere, this mixture was added into the Zn(OA)₂ solution at 80 °C. The reaction had the feed molar ratio of 4Zn to 1Se to 1DPP and the Se concentration of 60 mmol/kg. The total weight of the reaction mixture is 5.038 g with a Se concentration of 60 mmol/kg. The reaction temperature was increased, and nine samples were extracted after 15 min at 80, 100, 120, 140, 160, 180, 200, 220, and 240 °C. For the constant temperature model, it was stirred for 1 min and then heated directly to the target temperature. The sample was extracted after being maintained at this temperature for the corresponding time.

For the reactions with different feed concentrations (Fig. 3) and feed molar ratios (Fig. 4), all processes were the same. For the reaction batches with different reactivity (Fig. 5), all processes were the same except for the amount of DPP. A certain amount (such as 15 μL) of each as-synthesized sample was dispersed in the 3.0 mL of CH and in the mixture of 2.0 mL of CH and 1.0 mL of OTA for two minutes. The presence and evolution of MSC-299 were monitored mainly by UV-vis absorption spectroscopy.

Purification of MSC-299. A prenucleation stage sample was obtained by the reaction of 4Zn(OA)₂ + 1SeTOP + 1DPP in ODE performed at 160 °C for 30 min, with a feed concentration of 60 mmol/kg. The sample was stored at room temperature for a few days to precipitate the excess Zn(OA)₂. Then, 100 μL of the sample was added to a mixture of 100 μL Tol and 400 μL OLA, followed by the addition of 2.5 ml of MeCN. The mixtures were shaken and centrifuged at 9000 rpm for 2 min. The supernatant was removed, and the precipitate

was purified again in a similar way.

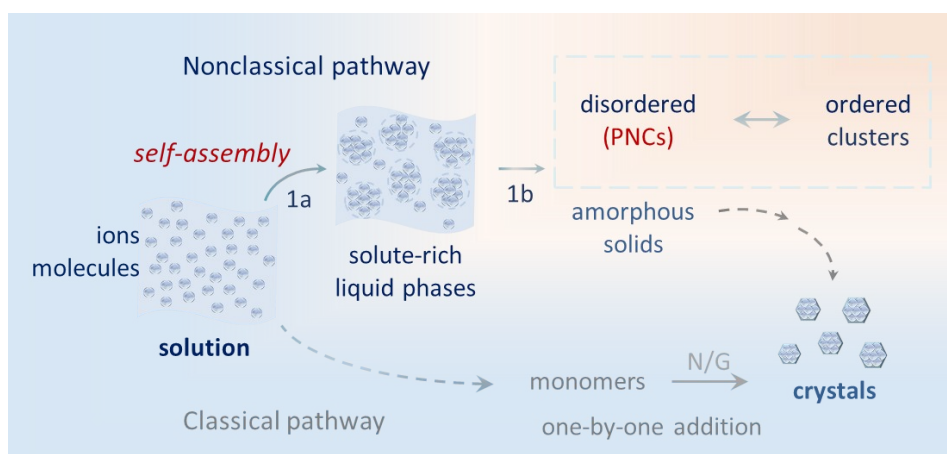
Transformation from ZnSe MSC-299 to MSC-320 and MSC-340. A prenucleation stage sample (preheated at 160 °C for 30 min) was purified by the method above. The resulting precipitate was completely dissolved in 1 mL of CH to obtain a solution. 200 µL of the solution was dispersed in the mixture of 2.795 mL of CH and 0.005 mL of MeOH. The transformation of MSCs was monitored mainly by UV-vis absorption spectroscopy.

Ultraviolet Absorption Spectroscopy. UV-vis absorption spectra were collected between 270 and 600 nm with an interval of 1 nm. Hitachi UH4150 and Hitachi U-2910 spectrometers were used. The quartz cuvettes (3.5 mL standard QS cells with the light path of 10 mm) were purchased from Hellma Analytics. Background measurements were performed with cyclohexane.

Matrix-Assisted Laser Desorption/Ionization Time-of-Flight Mass Spectrometry (MALDI-TOF MS). Shimadzu AXIMA Performance MALDI-TOF mass spectrometer was used (Fig. S2-2). Commercial 2,5-dihydroxyacetophenone (DHAP) was used as the matrix. 2.5 µL sample dispersion was mixed with 2.5 µL DHAP (from the mixture of 5 mg DHAP and 0.5 mL Tol). Then the mixture was dropped on a sample plate, and the measurement was carried out with a linear detector and positive mode. The ZnSe prenucleation-stage sample was synthesized at 160 °C/30 min by the feed molar ratio of 4Zn(OA)₂ to 1SeTOP to 1DPP with Se concentration of 60 mmol/kg. The as-synthesized sample was left at room temperature for 3 days to precipitate the excess Zn(OA)₂ and centrifuged at 9000 rpm for 2 min. After centrifugation, the precipitate was removed. For PC-299 (Fig. S2-2a), 150 µL of the supernatant was dispersed in 400 µL CH. For MSC-299 (Fig. S2-2b), 150 µL of the supernatant was dispersed in a mixture of 300 µL CH and 100 µL OTA.

Transmission Electron Microscope (TEM). TEM images were obtained on JEM-F200 (PC-299) and JEM-2100Plus (MSC-299). The sample of PC-299 is prepared in the same way as the sample of MALDI-TOF. The sample of MSC-299 was purified. For the preparation of the TEM grids, the samples of PC-299 and MSC-299 (Fig. S2-3) were dispersed in 3.0 mL of CH, respectively. Two drops of the resulting dispersion were placed on a TEM grid, which was

then dried under an ambient temperature.



Scheme S1. Generalization of the formation pathways for solids from solutions.¹⁻¹⁶ Until now, two models have been proposed to understand the nucleation pathway. One is the nonclassical pathway described in terms of multi-step nonclassical nucleation theory, which starts with self-assembly. The other is the classical pathway described by the single-step classical nucleation theory (CNT), which is assumed for the one-by-one addition of monomers. For the prenucleation stage of nonclassical pathway, “solute-rich liquid phases” seen (step 1a) in liquid-liquid phase separation,¹⁻⁷ and the presence of prenucleation clusters is observed in step 1b,^{1,6,8-11} also called as “amorphous solids” in some cases.^{4-5,13,14} Moreover, the transition of clusters from disorder (PNCs) to order clusters in the nonclassical pathway has been observed, which find analogue in the formation of QDs and MSCs.^{4-6,10,11,13-16}

- 1 J. T. Avaro, S. L. P. Wolf, K. Hauser and D. Gebauer, Stable Prenucleation Calcium Carbonate Clusters Define Liquid-Liquid Phase Separation. *Angew. Chem. Int. Ed.*, 2020, **59**, 6155–6159.
- 2 E. Wiedenbeck, M. Kovermann, D. Gebauer and H. Cölfen, Liquid Metastable Precursors of Ibuprofen as Aqueous Nucleation Intermediates. *Angew. Chem. Int. Ed.*, 2019, **58**, 19103–19109.
- 3 R. J. Davey, S. L. M. Schroeder and J. H. ter Horst, Nucleation of Organic Crystals - A Molecular Perspective. *Angew. Chem. Int. Ed.*, 2013, **52**, 2166–2179.
- 4 N. D. Loh, S. Sen, M. Bosman, S. F. Tan, J. Zhong, C. A. Nijhuis, P. Král, P. Matsudaira and U. Mirsaidov, Multistep Nucleation of Nanocrystals in Aqueous Solution. *Nat. Chem.*, 2017, **9**, 77–82.
- 5 B. Jin, Y. Wang, Z. Liu, A. France-Lanord, J. C. Grossman, C. Jin and R. Tang, Revealing the Cluster-Cloud and Its Role in Nanocrystallization. *Adv. Mater.*, **2019**, **31**, 1808225.
- 6 C. Yuan, A. Levin, W. Chen, R. Xing, Q. Zou, T. W. Herling, P. K. Challa, T. P. J. Knowles and X. Yan, Nucleation and Growth of Amino Acid and Peptide Supramolecular Polymers Through Liquid-Liquid Phase Separation. *Angew. Chem. Int. Ed.*, 2019, **58**, 18116–18123.

- 7 P. G. Vekilov, Dense Liquid Precursor for the Nucleation of Ordered Solid Phases from Solution. *Crystal Growth & Design*, 2004, **4**, 671–685.
- 8 D. Gebauer, A. Völkel and H. Coelfen, Stable Prenucleation Calcium Carbonate Clusters. *Science*, 2008, **322**, 1819–1822.
- 9 W. J. E. Habraken, M. J. Tao, L. J. Brylka, H. Friedrich, L. Bertinetti, A. S. Schenk, A. Verch, V. Dmitrovic, P. H. H. Bomans, P. M. Frederik, J. Laven, P. van der Schoot, B. Aichmayer, G. de With, J. J. DeYoreo and N. A. J. M. Sommerdijk, Ion-Association Complexes Unite Classical And Non-Classical Theories for the Biomimetic Nucleation of Calcium Phosphate. *Nat. Commun.*, 2013, **4**, 1507.
- 10 S. Jeon, T. Heo, S. Hwang, J. Ciston, K. C. Bustillo, B. W. Reed, J. Ham, S. Kang, S. Kim, J. Lim, K. Lim, J. S. Kim M., Kang, R. S. Bloom, S. Hong, K. Kim, A. Zettl, W. Y. Kim, P. Ercius, J. Park and W. C. Lee, Reversible Disorder-Order Transitions in Atomic Crystal Nucleation. *Science*, 2021, **371**, 498–503.
- 11 K. Cao, J. Biskupek, C. T. Stoppiello, R. L. McSweeney, T. W. Chamberlain, Z. Liu, K. Suenaga, S. T. Skowron, E. Besley, A. N. Khlobystov and U. Kaiser, Atomic Mechanism of Metal Crystal Nucleus Formation in A Single-Walled Carbon Nanotube. *Nat. Chem.*, 2020, **12**, 921–928.
- 12 H. Chen, M. Li, Z. Lu, X. Wang, J. Yang, Z. Wang, F. Zhang, C. Gu, W. Zhang, Y. Sun, J. Sun, W. Zhu and X. Guo, Multistep Nucleation and Growth Mechanisms of Organic S6 Crystals from Amorphous Solid States. *Nat. Commun.*, 2019, **10**, 3872.
- 13 J. Yang, J. Koo, S. Kim, S. Jeon, B. K. Choi, S. Kwon, J. Kim, B. H. Kim, W. C. Lee, W. B. Lee, H. Lee, T. Hyeon, P. Ercius and J. Park, Amorphous-Phase-Mediated Crystallization of Ni Nanocrystals Revealed by High-Resolution Liquid-Phase Electron Microscopy. *J. Am. Chem. Soc.*, 2019, **141**, 763–768.
- 14 R. Demichelis, P. Raiteri, J. D. Gale, D. Quigley and D. Gebauer, Stable Prenucleation Mineral Clusters Are Liquid-Like Ionic Polymers. *Nat. Commun.*, 2011, **2**, 590.
- 15 Y. Li, N. Rowell, C. Luan, M. Zhang, X. Chen and K. Yu, A Two-Pathway Model for the Evolution of Colloidal Compound Semiconductor Quantum Dots and Magic-Size Cluster. *Adv. Mater.*, 2022, **34**, 2107940.
- 16 L. Wang, J. Hui, J. Tang, N. Rowell, B. Zhang, T. Zhu, M. Zhang, X. Hao, H. Fan, J. Zeng, S. Han and K. Yu, Precursor Self-Assembly Identified as a General Pathway for Colloidal Semiconductor Magic-Size Clusters. *Adv. Sci.*, 2018, **5**, 1800632.

Table S1. Summary of hot-injection approaches to MSCs or QDs.

Refs (year)	Reactions	Growth T/t (°C/min)	Products ^a
1 (2005)	1Zn(C ₂ H ₅) ₂ /TOP-1SeTOP	300/1-5	MSC-328, 345
		300/20	QD-380
2 (2010)	1.5Zn(NA) ₂ -1H ₂ Se-OLA/OTA	220/4	MSC-328/347; QD-365
		220/120	QD-395
3 (2019)	Zn(OAc) ₂ ·7H ₂ O/OA-SeTOP	170/60	MSC-320; QD-350
		170/180	QD-375
4 (1993)	1.34Me ₂ Cd-1(TMS) ₂ Se	100	MSC-350, 415; QD-460
5 (2002)	2Cd-TDPA-1SeTBP	250/2	MSC-349
		250/4	MSC-349; QD-513
		250/60	QD-638
6 (2007)	1CdO/DDA-NA + 3.57SeTOP	80/100	MSC-350/360, 384, 406
		80/2500	QD-447
7 (2007)	1CdO/HPA + 1TeTOP	205-215/1	MSC-470, 505
		205-215/3	MSC-470, 505; QD-620
		205-215/8	QD-660
8 (2010)	2Cd(NA) ₂ -1TeTOP	130/6	MSC-445, 488, 506
		130/10	MSC-445, 488, 506; QD-520
		130/240	QD-575
9 (2023)	1.2Cd(OA) ₂ -1TeTOP	100/60	MSC-405/449
		100/1440	MSC-427/469; QD-510
10 (2013)	3Cd(OA) ₂ -1H ₂ S	260/10	MSC-311; QD-410
		260/60	QD-460
11 (2018)	2Cd(OA) ₂ -1STOP	130/360	MSC-324; QD-404
12 (2015)	2In(MA) ₃ -1P(SiPh ₃) ₃	150/60	MSC-386
		150/375	MSC-386; QD-510
		150/1085	QD-550

^a MSCs and QDs are labelled by their optical absorption wavelength.

Zn(NA)₂: zinc nonanote

Cd(NA)₂: cadmium nonanoic acid

NA: nonanoic acid	OLA: oleylamine
OTA: <i>n</i> -octylamine	TOP: tri- <i>n</i> -octylphosphine
TDPA: tetradecylphosphonic	TBP: tri- <i>n</i> -butylphosphine
(TMS) ₂ Se: bis(trimethylsilyl) selenium	HPA: <i>n</i> -hexylphosphonic acid
DDA: dodecylamine	OA: oleic acid
MA: myristic acid	

- 1 P. D. Cozzoli, L. Manna, M. L. Curri, S. Kudera, C. Giannini, M. Striccoli and A. Agostiano, Shape and Phase Control of Colloidal ZnSe Nanocrystals. *Chem. Mater.*, 2005, **17**, 1296–1306.
- 2 L. Zhang, X. Shen, H. Liang and J. Yao, Multiple Families of Magic-Sized ZnSe Quantum Dots via Noninjection One-Pot and Hot-Injection Synthesis. *J. Phys. Chem. C*, 2010, **114**, 21921–21927.
- 3 F. Baum, M. Fernandes da Silva, G. Linden, D. Feijo, E. S. Rieder and M. J. L. Santos, Growth Dynamics of Zinc Selenide Quantum Dots: the Role of Oleic Acid Concentration and Synthesis Temperature on Driving Optical Properties. *J. Nanopart. Res.*, 2019, **21**, 42.
- 4 C. B. Murray, D. J. Norris and M. G. Bawendi, Synthesis and Characterization of Nearly Monodisperse CdE (E = S, Se, Te) Semiconductor Nanocrystallites. *J. Am. Chem. Soc.*, 1993, **115**, 8706–8715.
- 5 Z. A. Peng and X. Peng, Nearly Monodisperse and Shape-Controlled CdSe Nanocrystals via Alternative Routes: Nucleation and Growth. *J. Am. Chem. Soc.*, 2002, **124**, 3343–3353.
- 6 S. Kudera, M. Zanella, C. Giannini, A. Rizzo, Y. Li, G. Gigli, R. Cingolani, G. Ciccarella, W. Spahl, W. J. Parak and L. Manna, Sequential Growth of Magic-Size CdSe Nanocrystals. *Adv. Mater.*, 2007, **19**, 548–552.
- 7 P. Dagtepe, V. Chikan, J. Jasinski and V. J. Leppert, Quantized Growth of CdTe Quantum Dots; Observation of Magic-Sized CdTe Quantum Dots. *J. Phys. Chem. C*, 2007, **111**, 14977–14983.
- 8 M. Zanella, A. Z. Abbasi, A. K. Schaper and W. J. Parak, Discontinuous Growth of II-VI Semiconductor Nanocrystals from Different Materials. *J. Phys. Chem. C*, 2010, **114**, 6205–6215.
- 9 S. A. Mech, F. Ma and C. Zeng, Mapping the Reaction Zones for CdTe Magic-Sized Clusters and their Emission Properties. *Nanoscale*, 2023, **15**, 114–121.
- 10 T. Yang, M. Lu, X. Mao, W. Liu, L. Wan, S. Miao and J. Xu, Synthesis of CdS Quantum Dots (QDs) via a Hot-Bubbling Route and Co-Sensitized Solar Cells Assembly. *Chem. Eng. J.*, 2013, **225**, 776–783.
- 11 D. R. Nevers, C. B. Williamson, B. H. Savitzky, I. Hadar, U. Banin, L. F. Kourkoutis, T. Hanrath and R. D. Robinson, Mesophase Formation Stabilizes High-Purity Magic-Sized Clusters. *J. Am. Chem. Soc.*, 2018, **140**, 3652–3662.
- 12 D. C. Gary, M. W. Terban, S. J. L. Billinge and B. M. Cossairt, Two-Step Nucleation and Growth of InP Quantum Dots via Magic-Sized Cluster Intermediates. *Chem. Mater.*, 2015, **27**, 1432–1441.

Table S2. Summary of heating-up approaches to MSCs or QDs.

Refs (year)	Reactions	Growth T/t (°C/min)	Products ^a
1 (2017)	4Cd(OAc) ₂ /OLA-1TeTOP	135/10	MSC-371
		135/40	MSC-371; QD-550
2 (2017)	4Cd(OA) ₂ -1S	180/15	MSC-311
		200/15	MSC-311; QD-375
3 (2018)	4Zn(OA) ₂ -1SeDPP	40/15	MSC-299
		60/15	MSC-299; QD-340
	4Zn(OA) ₂ -1SeTOP	200/15	MSC-299
		220/15	MSC-299; QD-375
		240/15	QD-390
4 (2022)	4ZnCl ₂ -8MPA-1SeU	RT/5	MSC-299
		RT/30	MSC-299; QD-340
5 (2022)	4Zn(OAc) ₂ /OLA-1SeTOP-1DPP	160/15	MSC-299
		220/15	QD-340
6 (2022)	4Cd(MA) ₂ -1SeTOP	180/15	MSC-373/393; MSC-433/460; QD-522
		240/15	QD-540
7 (2024)	3Cd(OAc) ₂ /OLA-1.5TeTOP-1DPP	100/15	MSC-351/372
		140/15	MSC-467/481; QD-554
		180/15	QD-645

^a MSCs and QDs are labelled by their optical absorption wavelength.

OLA: oleylamine

OA: oleic acid

MPA: 3-mercaptopropionic acid

TOP: tri-*n*-octylphosphine

DPP: diphenylphosphine

SeU: selenourea

- 1 M. Liu, K. Wang, L. Wang, S. Han, H. Fan, N. Rowell, J. A. Ripmeester, R. Renoud, F. Bian, J. Zeng and K. Yu, Probing Intermediates of the Induction Period Prior to Nucleation and Growth of Semiconductor Quantum Dots. *Nat. Commun.*, 2017, **8**, 15467.
- 2 T. Zhu, B. Zhang, J. Zhang, J. Lu, H. Fan, N. Rowell, J. A. Ripmeester, S. Han and K. Yu, Two-Step Nucleation of CdS Magic-Size Nanocluster MSC-311. *Chem. Mater.*, 2017, **29**, 5727–5735.

- 3 L. Wang, J. Hui, J. Tang, N. Rowell, B. Zhang, T. Zhu, M. Zhang, X. Hao, H. Fan, J. Zeng, S. Han and K. Yu, Precursor Self-Assembly Identified as a General Pathway for Colloidal Semiconductor Magic-Size Clusters. *Adv. Sci.*, 2018, **5**, 1800632.
- 4 Y. Li, M. Zhang, L. He, N. Rowell, T. Kreouzis, C. Zhang, S. Wang, C. Luan, X. Chen and K. Yu, Manipulating Reaction Intermediates to Aqueous-Phase ZnSe Magic-Size Clusters and Quantum Dots at Room Temperature. *Angew. Chem. Int. Ed.*, 2022, **61**, e202209615.
- 5 X. Yang, M. Zhang, Q. Shen, Y. Li, C. Luan and K. Yu, The Precursor Compound of Two Types of ZnSe Magic-Sized Clusters. *Nano Res.*, 2022, **15**, 465–474.
- 6 J. Shen, C. Luan, N. Rowell, Y. Li, M. Zhang, X. Chen and K. Yu, Size Matters: Steric Hindrance of Precursor Molecules Controlling the Evolution of CdSe Magic-Size Clusters and Quantum Dots. *Nano Res.*, 2022, **15**, 8564-8572.
- 7 Z. Wang, C. Zhang, S. Wang, M. Zhang, X. Chen, C. Luan and K. Yu, Formation and Transformation of ZnTe and CdTe Magic-Size Clusters Assisted by Their Precursor Compounds. *Chem. Mater.*, 2024, **36**, 2520–2532.

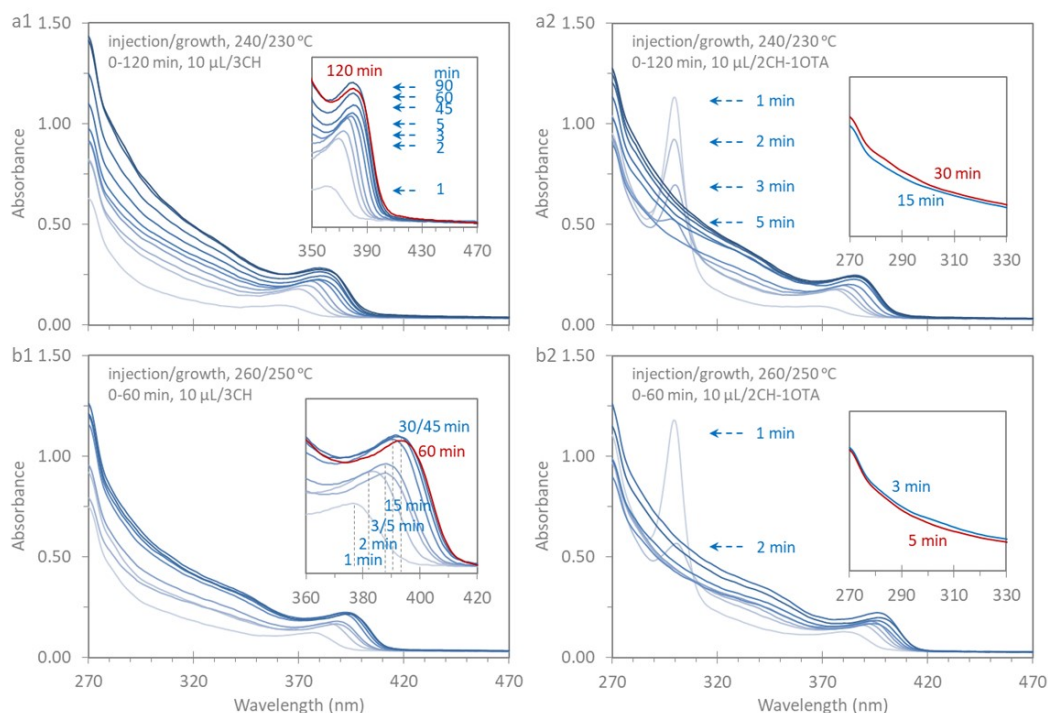


Fig. S1-1. Absorption spectra of the samples from the two reactions of Fig. 1. For the top panel, ten samples were extracted at 1, 2, 3, 5, 15, 30, 45, 60, 90, and 120 min. For the bottom panel, eight samples were extracted at 1, 2, 3, 5, 15, 30, 45, and 60 min. An aliquot (10 μL) of each sample was dispersed in 3.0 mL of CH (a1 and b1) and in 2CH-10TA (a2 and b2) for the measurement of optical absorption measurement.

- (a1) The nucleation and growth (N/G) of QDs occurred immediately after injection the mixture of SeTOP and DPP and grew within 120 min. Inset features the QDs growth. (a2) PC-299 formed and reached its maximum at 1 min. Then PC-299 decreased and disappeared at 15 min. Inset highlights the absence of MSC-299 after 15 min.
- (b1) QDs formed immediately after injection and grew within 60 min. Inset features the QDs growth. (b2) PC-299 formed immediately after the injection and reached its maximum at 1 min. Then PC-299 decreased and disappeared at 3 min. Inset highlights the absence of MSC-299 after 3 min.

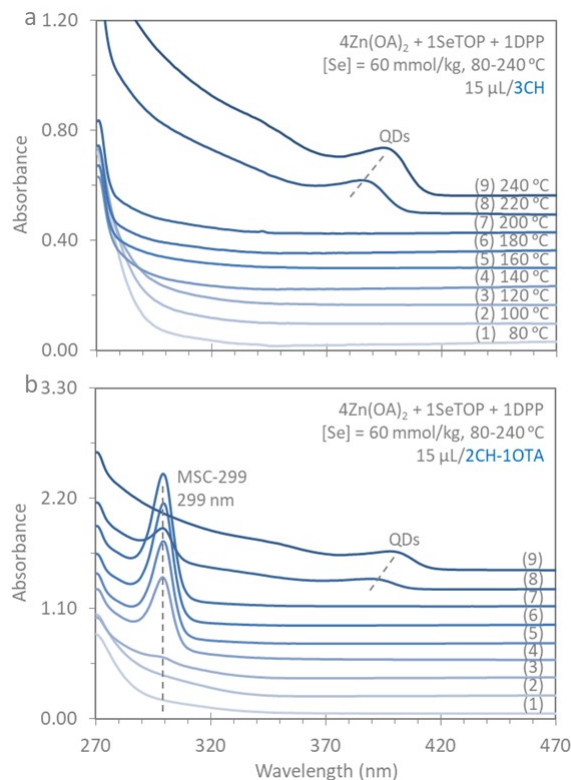


Fig. S2-1. Absorption spectra of the samples from the reaction of Fig. 2. Reaction of $4\text{Zn}(\text{OA})_2 + 1\text{SeTOP} + 1\text{DPP}$ ($[\text{Se}] = 60 \text{ mmol/kg}$) was heated from 80 to 240 °C with steps of 20 °C, and nine samples were extracted at each temperature step after 15 min elapses. For the measurement, 15 μL of each sample was dispersed in 3.0 mL of CH (a) and in 2CH-10TA (b).

- (a) QDs were not seen in the first seven samples (traces 1 to 7), appeared at 220 °C (trace 8), and redshifted at 240 °C (trace 9).
- (b) MSC-299 formed at 120 °C (trace 3), reaching its maximum at 200 °C (trace 7). Then MSC-299 decreased at 220 °C (trace 8) and disappeared at 240 °C (trace 9). Similarly, QDs were seen for the last two samples (traces 8 to 9).
- For the reaction, the prenucleation cluster PC-299 formed at 120 °C and increased until 200 °C. The prenucleation stage was below 200 °C; the N/G of QDs occurred at 220 °C.

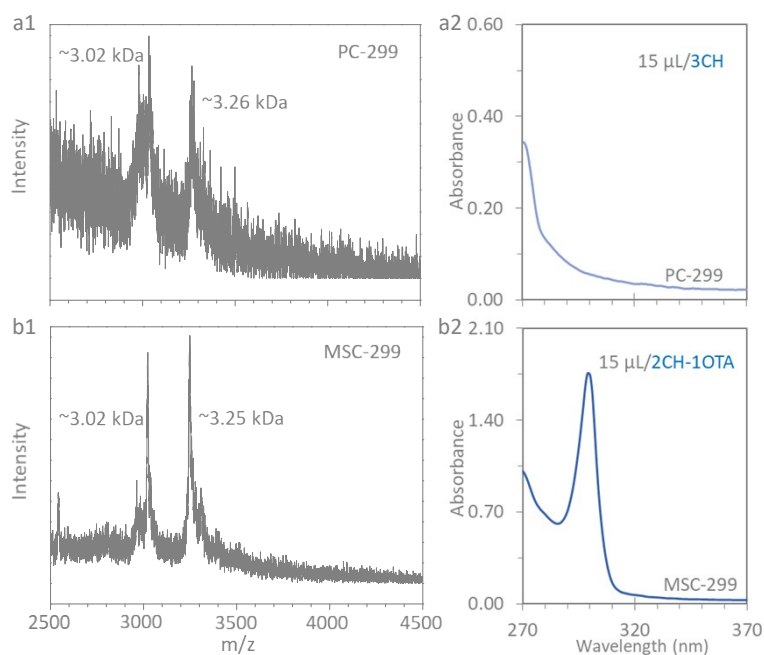


Fig. S2-2. MALDI-TOF MS of PC-299 and MSC-299. A prenucleation-stage sample of ZnSe (160 °C/30 min) was obtained from the reaction of Fig. S2-1. The as-synthesis sample was kept at room temperature for 3 days to precipitate the excess Zn(OA)₂, and then centrifuged with a speed of 9000 rpm for 2 min. Subsequently, the precipitate was removed.

- For PC-299 (top panel), the supernatant (150 μL) was dispersed in 400 μL CH for the measurement of MALDI-TOF MS (a1). 15 μL of the supernatant was dispersed in 3 mL of CH for the measurement of optical absorption (a2).
- For MSC-299 (bottom panel), the supernatant (150 μL) was dispersed in the mixture of 300 μL CH and 100 μL OTA for the measurement of MALDI-TOF MS (b1). 15 μL of the supernatant was dispersed in 2CH-1OTA for the measurement of optical absorption (b2).
- The m/z range of MALDI-TOF MS is from 2500 to 4500 Da. MSC-299 was detected in the CH-OTA mixture but not in CH, which is the evidence of the existence of PC-299. The core masses of PC-299 and MSC-299 are similar, which supports the fact that PC-299 and MSC-299 are a pair of isomers. A composition of Zn₃₂Se₁₅ is thus assumed, according to our previous study.¹

[1] X. Yang, M. Zhang, Q. Shen, Y. Li, C. Luan and K. Yu, The Precursor Compound of Two Types of ZnSe Magic-Sized Clusters. *Nano Res.*, 2022, **15**, 465–474.

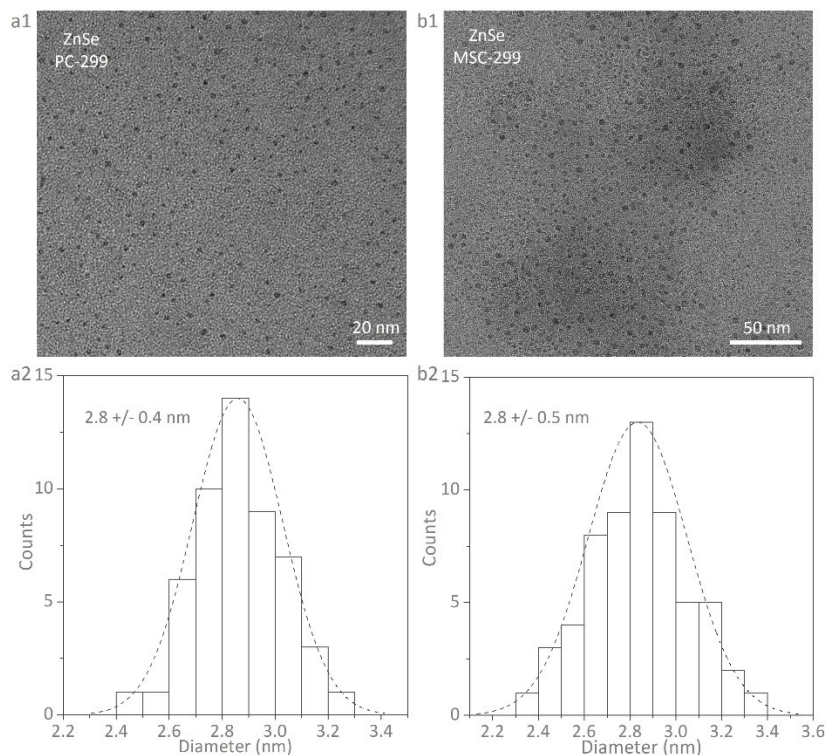


Fig. S2-3. TEM images of PC-299 and MSC-299, with corresponding size analysis.

- For PC-299 (a1), a prenucleation-stage sample of ZnSe (160 °C/30 min) was obtained from the reaction of Fig. S2-1. The as-synthesis sample was kept at room temperature for 3 days to precipitate the excess Zn(OA)₂, then centrifuged with a speed of 9000 rpm for 2 min. Subsequently, the precipitate was removed. The supernatant (40 μL) was dispersed 3.0 mL of CH. For the particles shown in part a1, 50 clusters were used for size analysis (a2). The fitted curve (dashed line) has Gaussian distribution, yielding the size of 2.8 ± 0.4 nm for PC-299.
- For MSC-299 (b1), the prenucleation-stage sample of ZnSe (160 °C/30 min) was purified with OLA, Tol and MeCN. Subsequently, the purified sample was dissolved in 200 μL of CH, and 100 μL of which was dispersed in 3.0 mL of CH. For the particles shown in part b1, 60 clusters were used for size analysis (b2). The fitted curve (dashed line) has Gaussian distribution, yielding the size of 2.8 ± 0.5 nm for MSC-299.
- TEM results suggest that PC-299 and MSC-299 are dot-like with similar sizes. We propose that PC-299 and MSC-299 are a pair of isomers, which should have the same composition but different structure.

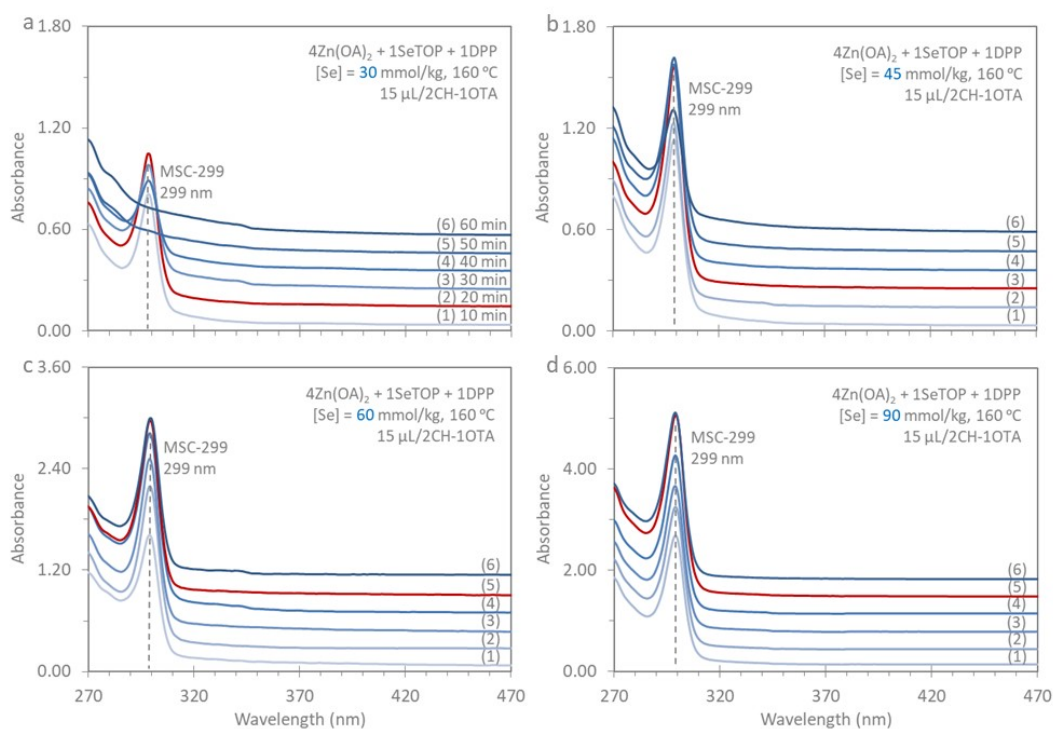


Fig. S3-1. Optical absorption spectra of the samples from the four Fig. 3a reactions. The reactions of $4\text{Zn}(\text{OA})_2 + 1\text{SeTOP} + 1\text{DPP}$ with different Se concentrations of 30 (a), 45 (b), 60 (c), and 90 mmol/kg (d) were heated and kept at 160 °C. From each reaction, six samples were extracted from 10 to 60 min with an interval of 10 min as indicated. Each 15 μL of the sample was dispersed in 2CH-1OTA for the measurement. The red traces represent the absorption spectra of the maximum OD value for each reaction. MSC-299 was seen in the four reactions. The OD of MSC-299 is obtained from the optical strength at 299 nm subtracted by that at 320 nm. The maximum OD of MSC-299 (red traces) was 0.81 at 20 min (a), 1.22 at 30 min (b), 1.89 at 50 min (c), and 3.33 at 50 min (d).

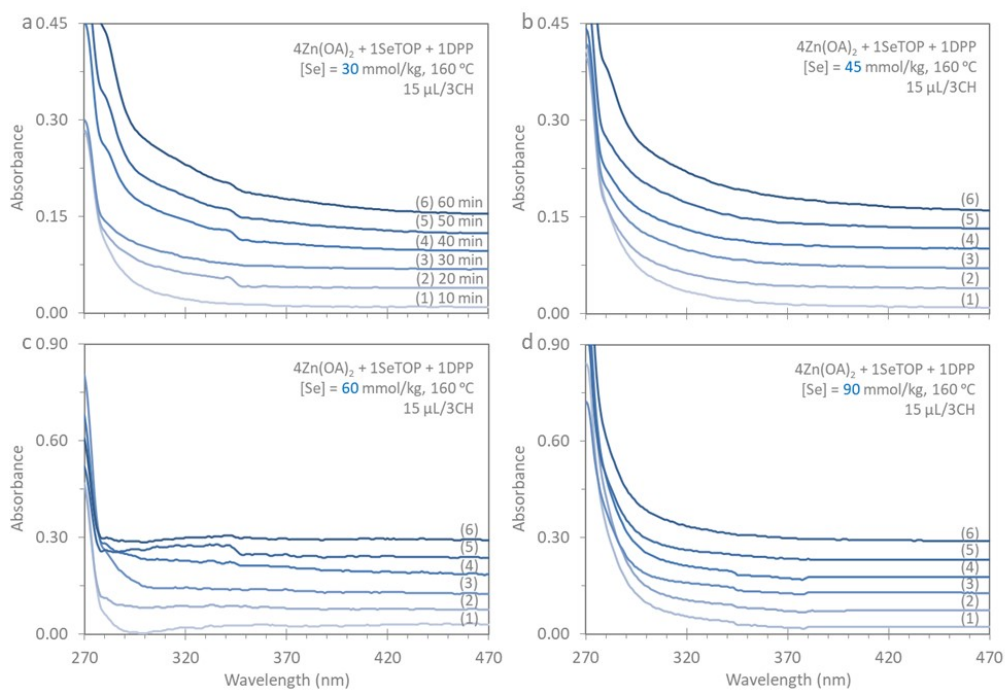


Fig. S3-2. Optical absorption spectra of the samples in CH from the reactions in Fig. S3-1. Each 15 μL of the sample was dispersed in 3.0 mL of CH for the measurement of optical absorption. MSC-299 was not seen in the four reactions.

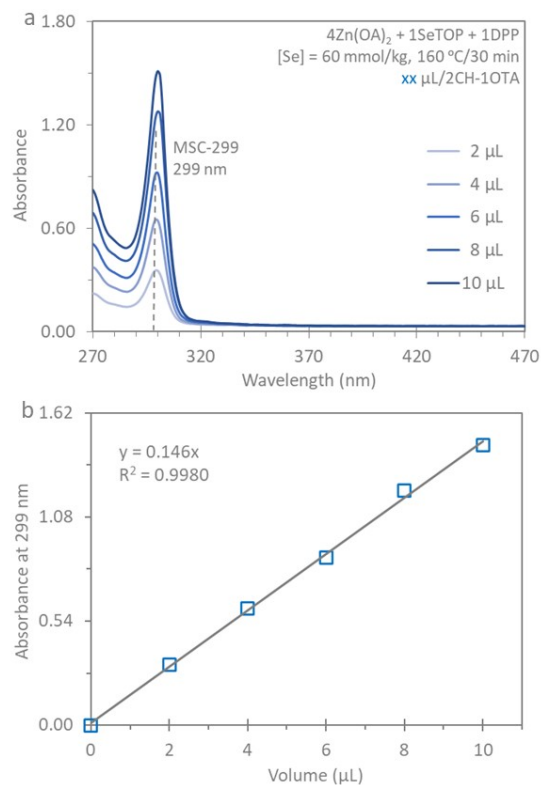


Fig. S3-3. Concentration-dependent absorption of MSC-299. The prenucleation stage sample was prepared at 160 °C for 30 min from a similar reaction for Fig. S3-1c. With the amount of 2, 4, 6, 8, and 10 μL, the sample was dispersed in 2CH-10TA for the optical absorption measurement (a). The absorption strength at 299 nm for MSC-299 (y axis) was plotted as a function of the sample volume (μL) (x axis) (b). A linear relationship between the MSC-299 amount and the sample volume was obtained, $y = 0.146x$, $R^2=0.9980$. Thus, the MSC-299 amount can be used to indicate the PC-299 amount in the sample.

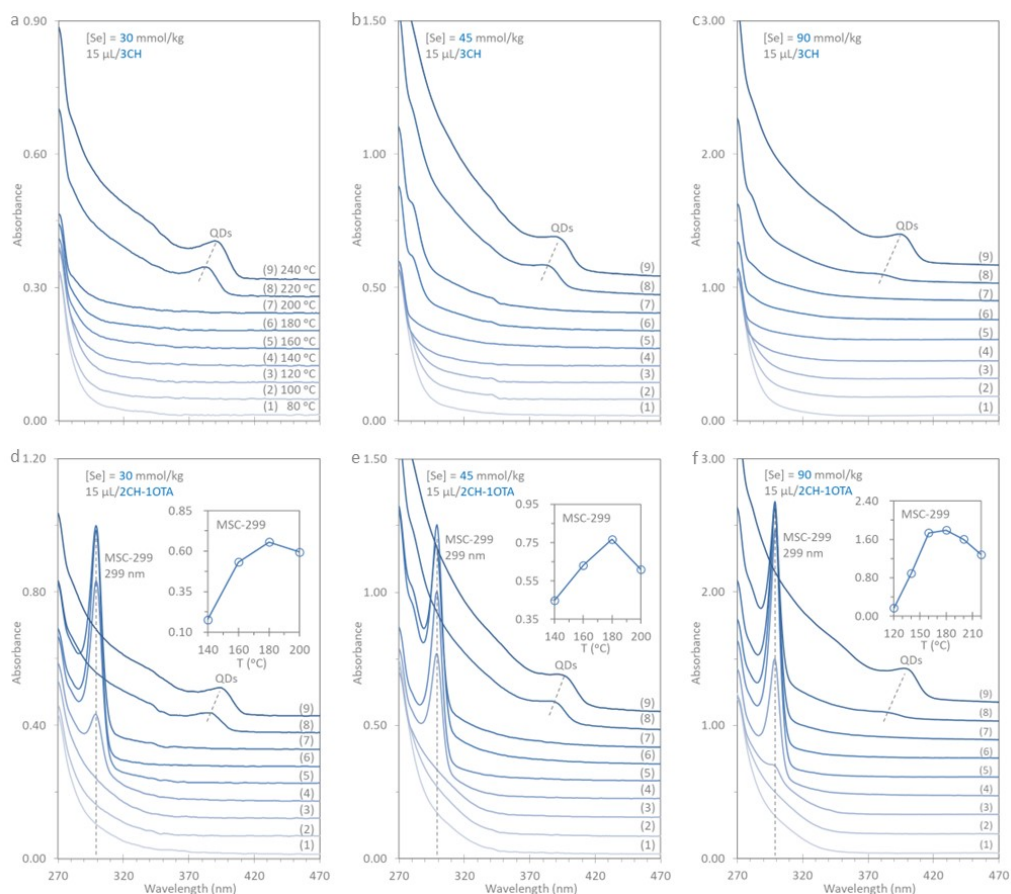


Fig. S3-4. Absorption spectra of the samples from three reactions of $4\text{Zn}(\text{OA})_2 + 1\text{SeTOP} + 1\text{DPP}$ with different feed concentrations. The Se concentrations were 30, 45, and 90 mmol/kg, respectively. When the temperature was increased from 80 to 240 °C with steps of 20 °C, nine samples (15 μL) were extracted and dispersed in 3.0 mL of CH (top panel) and 2CH-10TA (bottom panel) for the absorption measurement. The insets show the trend of changes in MSC-299 amount (bottom panel).

- In CH, QDs appeared at 220 °C, and redshifted at 240 °C.
- In the CH-OTA mixture, MSC-299 was observed at 120 °C (90 mmol/kg) or 140 °C (30 and 45 mmol/kg), while QDs were observed at 220 °C. The OD value of MSC-299 increased with the increase of feed concentration.
- The MSC-299 strength indicates the PC-299 amount. High feed concentrations facilitate the formation of PC-299. When the concentration was 45 mmol/kg, MSC-299 was also can be detected at 120 °C (Fig. S3-5).

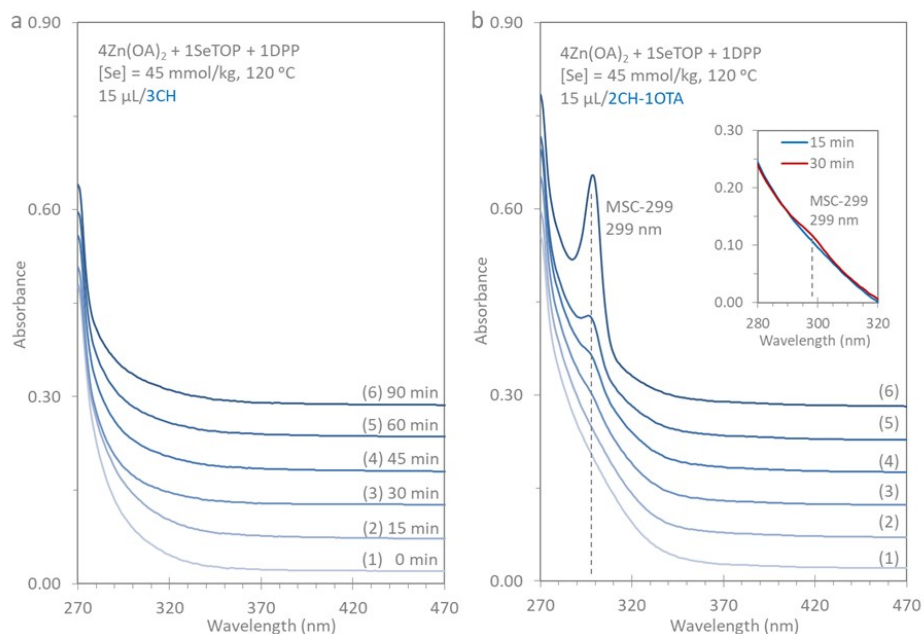


Fig. S3-5. The temporal evolution of MSC-299 from the reaction of $4\text{Zn}(\text{OA})_2 + 1\text{SeTOP} + 1\text{DPP}$ at $120\text{ }^\circ\text{C}$. The reaction had a Se feed concentration of 45 mmol/kg . Six samples were extracted within 90 min as indicated. $15\text{ }\mu\text{L}$ of each sample was dispersed in 3.0 mL of CH (a) and 2CH-10TA (b) for the optical absorption measurement. The inset is the expanded view of 15 (trace 2) and 30 min (trace 3) samples in Part b.

- (a) In CH, no clusters or QDs were observed.
- (b) In the CH-OTA mixture, MSC-299 appeared in the 30 min sample (trace 3), and increased over time. Inset highlights the absence of MSC-299 at 30 min (red trace).

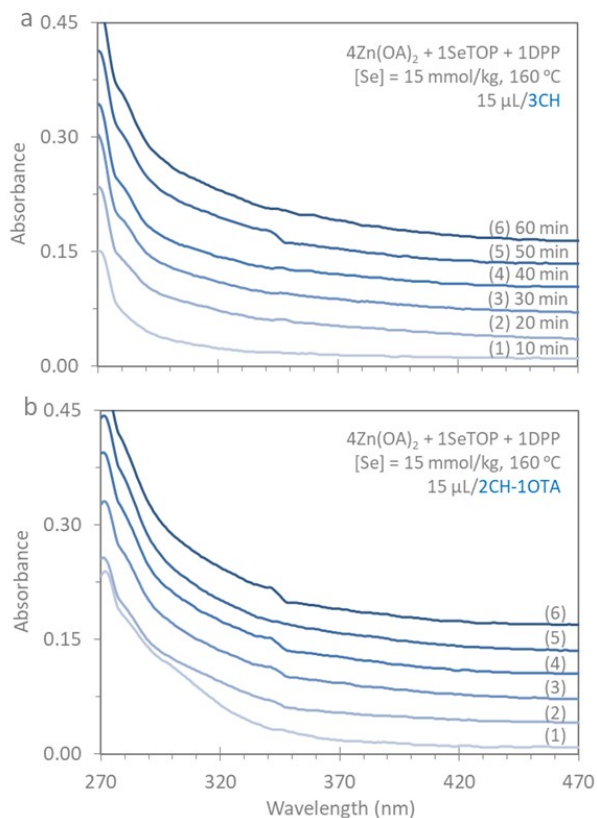


Fig. S3-6. The temporal evolution of MSC-299 from the reaction of $4\text{Zn}(\text{OA})_2 + 1\text{SeTOP} + 1\text{DPP}$ at 160°C . The reaction had a Se feed concentration of 15 mmol/kg . Six samples were extracted from 10 to 60 min with an interval of 10 min as indicated. $15 \mu\text{L}$ of each sample was dispersed in 3.0 mL of CH (a) and 2CH-10TA (b) for the optical absorption measurement.

- (a) In CH, no clusters or QDs were observed.
- (b) In the CH-OTA mixture, no clusters or QDs were observed.
- We argue that the formation of “micellar-like” aggregates (self-assembly, Step 1a) requires a SeTOP concentration higher than 15 mmol/kg .

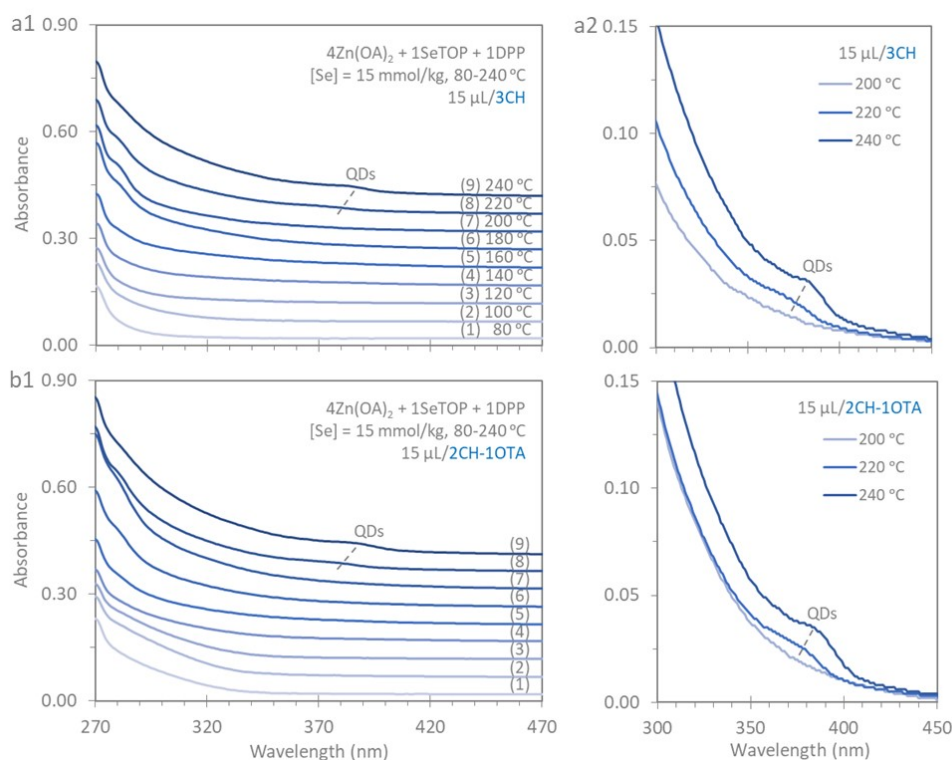


Fig. S3-7. Absorption spectra of the samples from the reaction of $4\text{Zn}(\text{OA})_2 + 1\text{SeTOP} + 1\text{DPP}$ with a Se concentration of 15 mmol/kg. When the temperature was increased from 80 to 240 °C with steps of 20 °C, nine samples (15 μL) were extracted at each temperature and dispersed in 3.0 mL of CH (a1) and 2CH-10TA (b1) for optical absorption measurement. Parts a2 and b2 are expanded views of 200, 220, and 240 °C (traces 7, 8, and 9) samples in Parts a1 and b1, respectively.

- No clusters were seen. QDs appeared at 220 °C (trace 8), and redshifted at 240 °C (trace 9).
- The Se feed concentration of 15 mmol/kg is lower than the critical concentration for self-assembly.

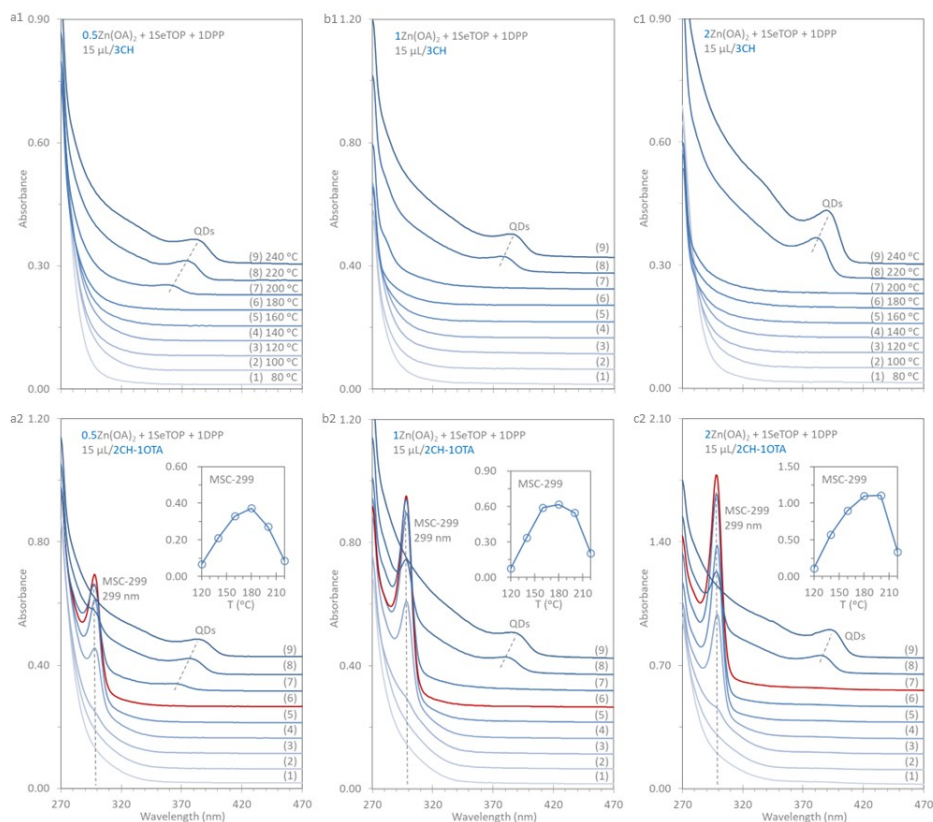


Fig. S4-1. Absorption spectra of the samples from reactions with different feed molar ratios.

Three reactions were performed with the feed molar ratio of $0.5/1/2\text{Zn(OA)}_2 + 1\text{SeTOP} + 1\text{DPP}$ and the Se concentration of 60 mmol/kg in ODE. When the temperature was increased from 80 to 240 °C with steps of 20 °C, nine samples (15 μL) were extracted at each temperature and dispersed in 3.0 mL of CH (top panel) and 2CH-1OTA (bottom panel) for optical absorption measurement. The insets show the changing trend of MSC-299 amount (bottom panel). The red traces represent the absorption spectra of the maximum OD value for each reaction.

- In CH (top panel), no clusters were observed for the first seven samples (traces 1 to 7). The N/G of QDs occurred at 200 °C (trace 7, a1) or 220 °C (trace 8, b1 and c1), and redshifted at 240 °C (trace 9).
- In the CH-OTA mixture (bottom panel), MSC-299 was seen at 140 °C (trace 4, a2) or 120 °C (trace 3, b2 and c2) and reached its maximum at 180 °C (trace 6, a2 and b2) or 200 °C (trace 7, c2).

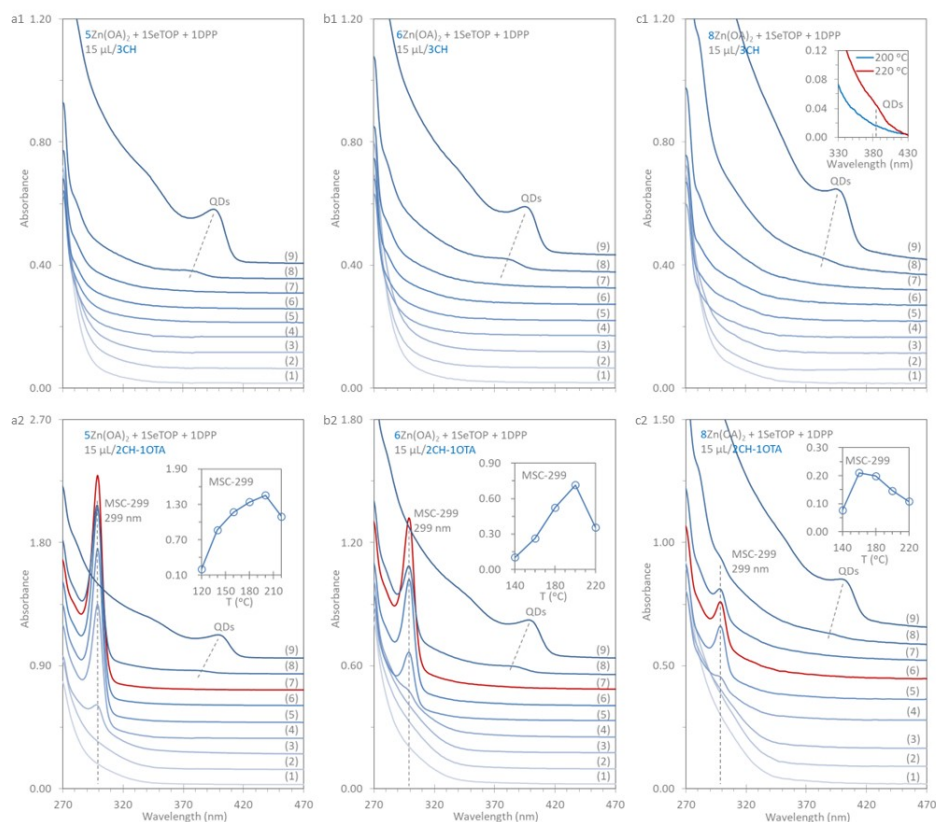


Fig. S4-2. Absorption spectra of the samples from the reactions with different feed molar ratios. Three reactions are performed with the feed molar ratio of $5/6/8\text{Zn}(\text{OA})_2 + 1\text{SeTOP} + 1\text{DPP}$ and the Se concentration of 60 mmol/kg in ODE. When the temperature was increased from 80 to 240 °C with steps of 20 °C, nine samples (15 μL) were extracted at each temperature and dispersed in 3.0 mL of CH (top panel) and 2CH-1OTA (bottom panel) for optical absorption measurement. The inset in Part c1 shows the expanded view of 200 and 220 °C (traces 7 and 8) samples. The insets in bottom panel show the changing trend of MSC-299 amount. The red traces represent the absorption spectra of the maximum OD value for each reaction. The results are similar to Fig. S4-1.

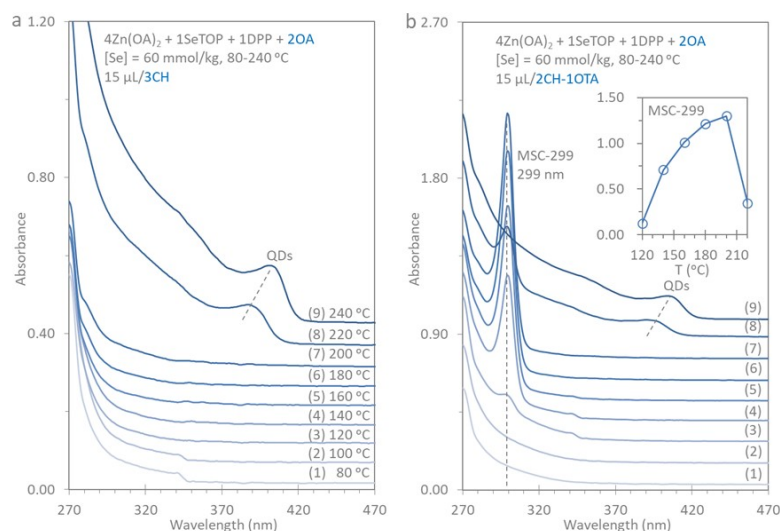


Fig. S4-3. Effect of additional OA on the formation of MSC-299 studied by optical absorption spectroscopy. The feed molar ratio of the reaction was $4\text{Zn}(\text{OA})_2 + 1\text{SeTOP} + 1\text{DPP}$ with the Se concentration of 60 mmol/kg in ODE. A small amount of oleic acid (OA, 0.370 g) was added before SeTOP. ODE was added to keep the total weight of about 5.000 g. When the temperature was increased from 80 to 240 °C with steps of 20 °C, nine samples (15 μL) were extracted at each temperature and dispersed in 3.0 mL of CH (a) and 2CH-1OTA (b) for optical absorption measurement. The inset in Part b shows the changing trend of MSC-299 amount.

- (a) In CH, no clusters were observed for the first seven samples (traces 1 to 7). QDs appeared at 220 °C (trace 8) and redshifted at 240 °C (trace 9).
- (b) In the CH-OTA mixture, MSC-299 was seen at 120 °C (trace 3), kept increasing until 200 °C (trace 7), decreased at 220 °C (trace 8), and disappeared at 240 °C (trace 9). QDs were seen at 220 °C (trace 8).
- Compared with the reaction without additional OA, the yield of MSC-299 does not decrease. The addition of OA will not suppress the production of MSC-299.

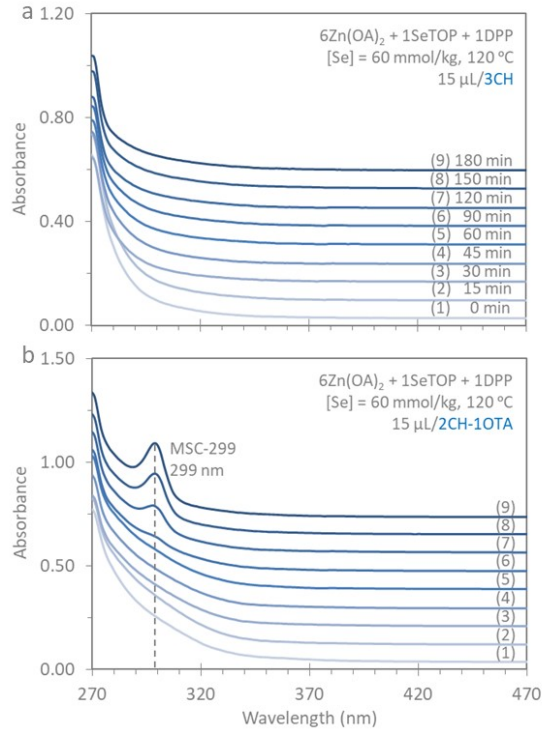


Fig. S4-4. The temporal evolution of MSC-299 from the reaction of $6\text{Zn}(\text{OA})_2 + 1\text{SeTOP} + 1\text{DPP}$ at $120\text{ }^\circ\text{C}$. The reaction had a Se concentration of 60 mmol/kg . Nine samples were extracted within 180 min as indicated. $15\text{ }\mu\text{L}$ of each sample was dispersed in 3.0 mL of CH (a) and 2CH-1OTA (b).

- (a) In CH, no clusters or QDs were observed.
- (b) In the CH-OTA mixture, MSC-299 appeared in the 90 min sample (trace 6), and increased over time.

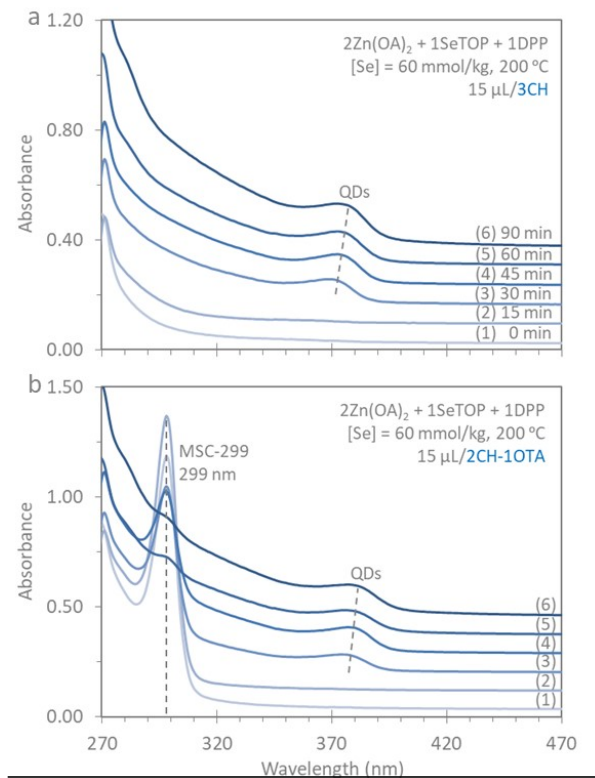


Fig. S4-5. The temporal evolution of MSC-299 from the reaction of $2\text{Zn}(\text{OA})_2 + 1\text{SeTOP} + 1\text{DPP}$ at $200\text{ }^\circ\text{C}$. The reaction had a Se concentration of 60 mmol/kg . Six samples were extracted from 0 to 90 min as indicated. Each $15\text{ }\mu\text{L}$ of the sample was dispersed in 3.0 mL of CH (a) and 2CH-1OTA (b).

- (a) In CH, no clusters were seen for the first two samples (traces 1 to 2). QDs appeared at 30 min (trace 3) and redshifted until 90 min (trace 6).
- (b) In the CH-OTA mixture, MSC-299 appeared immediately and reached its maximum at 15 min. Then MSC-299 kept decreasing over time. The N/G of QDs occurred for the 30 min sample (trace 3).

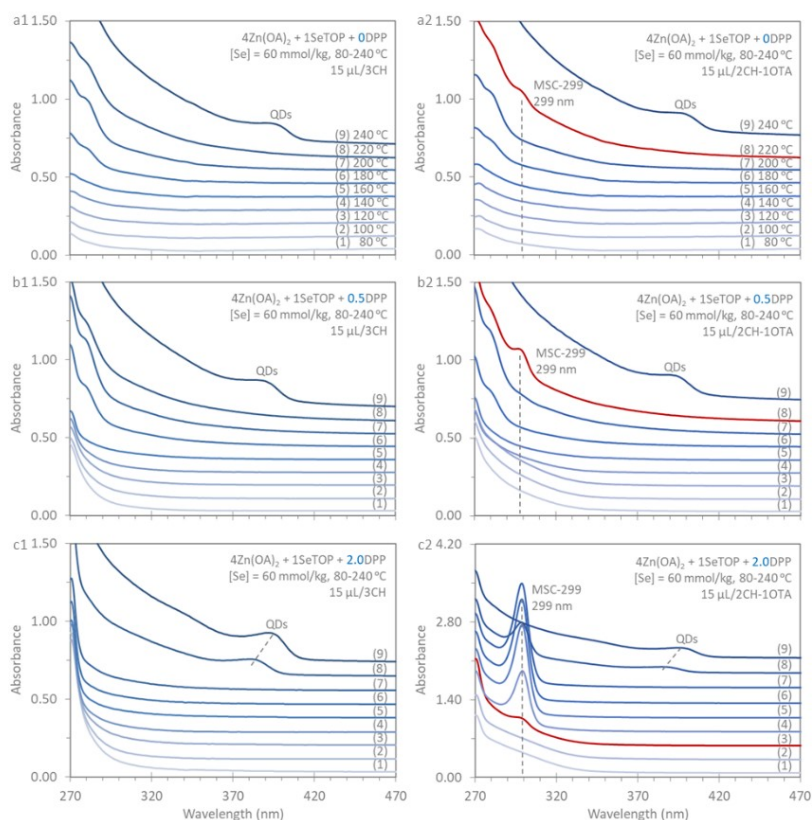


Fig. S5-1. Absorption spectra of the samples from the reaction of Fig. 5. Three reactions of $4\text{Zn}(\text{OA})_2 + 1\text{SeTOP} + x\text{DPP}$ ($x = 0/0.5/2.0$) were performed the Se feed concentration of 60 mmol/kg. Each reaction was heated from 80 to 240 °C with steps of 20 °C; each nine samples were extracted after holding for 15 min at each temperature. Each 15 μL of the sample was dispersed in 3.0 mL of CH (left panel) and in 2CH-1OTA (right panel) for the measurement of optical absorption.

- In CH (left panel), No clusters were seen in the three reactions. QDs appeared at 240 °C (trace 9, a1 and b1) or 220 °C sample (trace 8, c1).
- In the CH-OTA mixture (right panel), the red traces represented the absorption spectra of the sample in which MSC-299 first appeared. When the ratio of DPP is 0 (a2) or 0.5 (b2), MSC-299 was observed in the 220 °C samples (trace 8), and QDs appeared in the 240 °C samples (trace 9). When the ratio of DPP is 2 (c2), MSC-299 was seen in the samples from 120 (trace 3) to 220 °C (trace 8), and QDs were seen for the last two samples (traces 8 to 9).

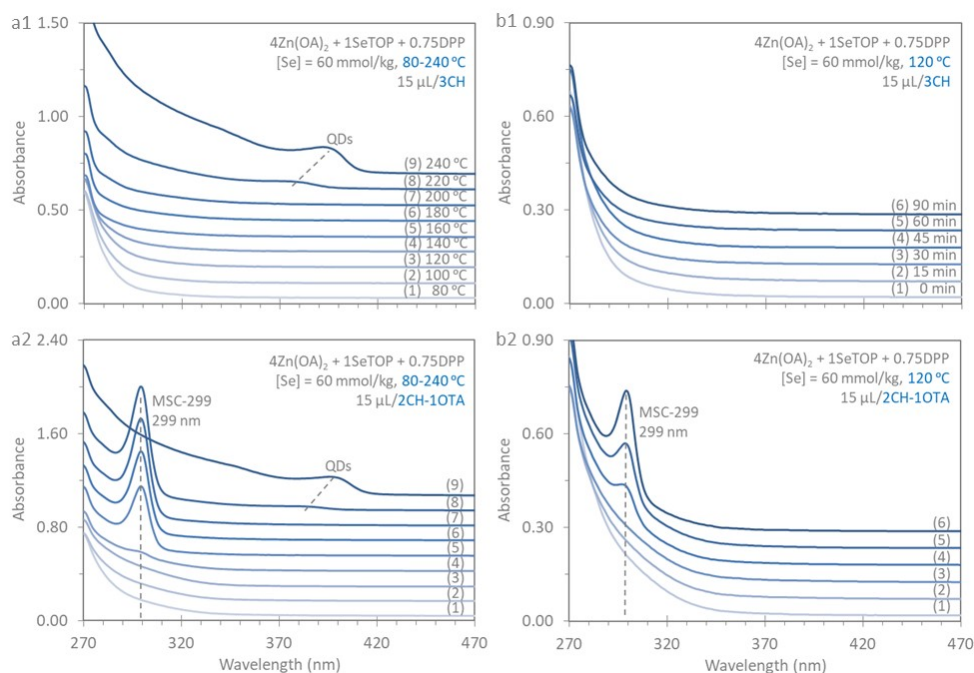


Fig. S5-2. Effect of DPP amount on the formation of PC-299 studied by optical absorption spectroscopy. The reaction of $4\text{Zn}(\text{OA})_2 + 1\text{SeTOP} + 0.75\text{DPP}$ were performed, with the Se feed concentration of 60 mmol/kg. 15 μL of each sample was dispersed in 3.0 mL of CH (a1 and b1) and in 2CH-1OTA (a2 and b2) for optical absorption measurement.

- For Parts a1 and a2, the reaction was heated from 80 to 240 °C with steps of 20 °C; nine samples were extracted after holding for 15 min at each temperature. In CH, no clusters were observed for the first seven samples (traces 1 to 7). The N/G of QDs occurred at 220 °C (trace 8), and redshifted at 240 °C (trace 9). In the CH-OTA mixture, MSC-299 was seen at 140 °C and reached its maximum at 220 °C.
- For Parts b1 and b2, the reaction was kept at 120 °C, and six samples were within 90 min. In CH, no clusters or QDs were observed. In the CH-OTA mixture, MSC-299 appeared in the 45 min sample (trace 4), and increased over time.
- MSC-299 was seen at 120 °C, indicating the formation of Zn–Se bonds.

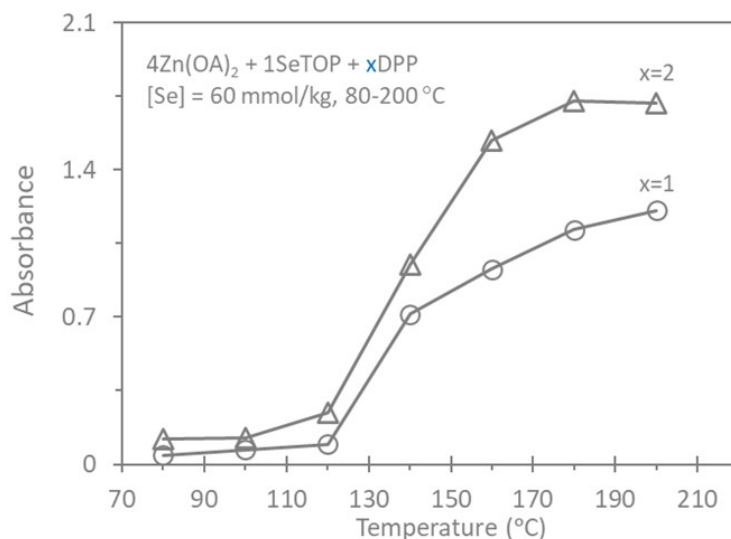


Fig. S5-3. Variation of the OD value of MSC-299. Two reactions of $4\text{Zn}(\text{OA})_2 + 1\text{SeTOP} + x\text{DPP}$ ($x = 1$ (circles) or $x = 2$ (triangles)) were performed, with the Se feed concentration of 60 mmol/kg. Each reaction was heated from 80 to 200 °C with steps of 20 °C; each seven samples were extracted after holding for 15 min at each temperature. 15 μL ($x = 1$) or 10 μL ($x = 2$) of each sample was dispersed in a mixture of 2CH-1OTA for the measurement of optical absorption. The OD values of the samples from $x = 2$ reaction was increased to uniform the volume (15 μL). The OD value of MSC-299 increased with the amount of DPP. We argue that the increase in the amount of DPP shifts the balance ($\text{SeTOP} + \text{DPP} \rightleftharpoons \text{TOP} + \text{SeDPP}$) to the right, and more SeDPP are obtained to participate in self-assembly (Step 1a). Thus, the usage of DPP favors the formation of PC-299.

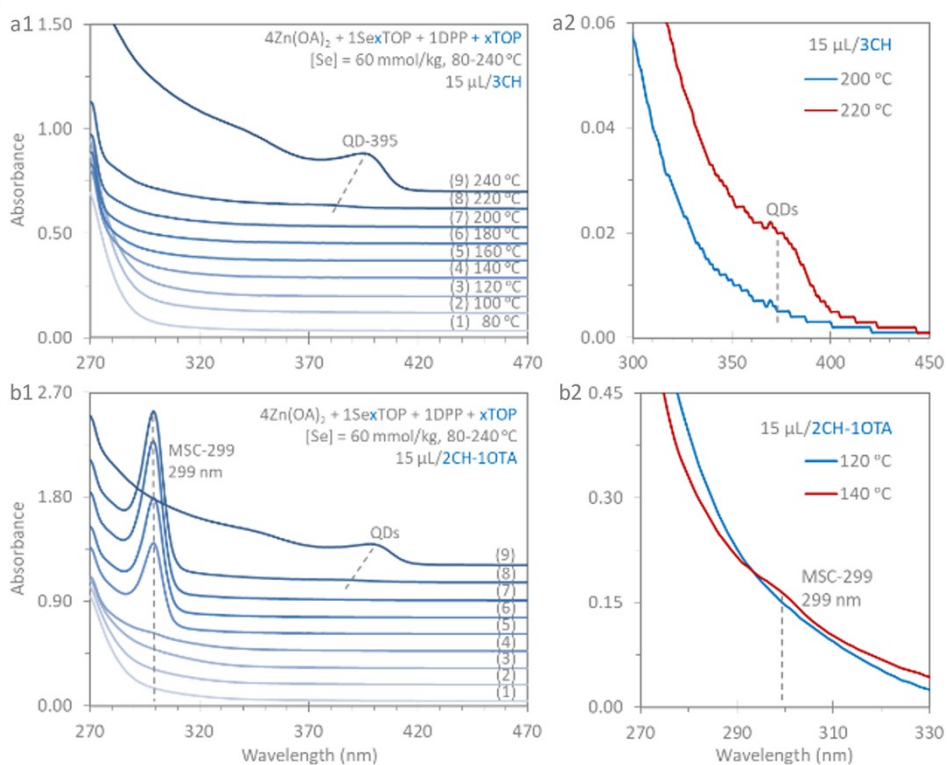


Fig. S5-4. Effect of additional TOP on the formation of MSC-299 studied by optical absorption spectroscopy. The feed molar ratio of the reaction was $4\text{Zn}(\text{OA})_2 + 1\text{SeTOP} + 1\text{DPP} + x\text{TOP}$ with the Se concentration of 60 mmol/kg in ODE. A small amount of TOP (0.247 g) was added together with SeTOP, and then ODE was added to keep the total weight of about 5.000 g. When the temperature was increased from 80 to 240 °C with steps of 20 °C, nine samples (15 μL) were extracted at each temperature after 15 min elapses and dispersed in 3.0 mL of CH (a1) and 2CH-10TA (b1) for optical absorption measurement. Part a2 is the expanded view of 200 and 220 °C (traces 7 and 8) samples in Part a1. Part b2 is the expanded view of 120 and 140 °C (traces 3 and 4) samples in Part b1.

- (a) In CH, no clusters were observed for the first seven samples (traces 1 to 7). QDs appeared at 220 °C (trace 8).
- (b) In the CH-OTA mixture, MSC-299 was seen at 140 °C (trace 4). QDs were seen at 220 °C (trace 8).
- Compared with the reaction without additional TOP, the yield of MSC-299 decreases. Thus, the addition of TOP facilitates the shift of the balance ($\text{SeTOP} + \text{DPP} \rightleftharpoons \text{TOP} + \text{SeDPP}$) to the left, and reduces the amount of available SeDPP in the reaction.

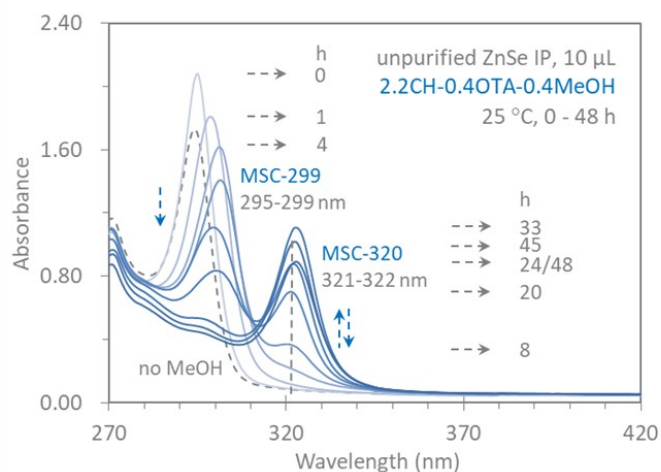


Fig. S6-1. Transformation of unpurified MSC-299 at room temperature studied by optical absorption spectroscopy. A prenucleation stage sample was prepared at 160 °C for 30 min from a similar reaction for Fig. S3-1c.

- 10 μL of the sample was first dispersed in 2.2CH-0.4OTA (gray dashed line). MSC-299 was observed.
- 0.4 mL MeOH was added to the dispersion; nine spectra were extracted at 0, 1, 4, 8, 20, 24, 33, 45, and 48 h. At 0 h, the strength of MSC-299 increased. The strength of MSC-299 decreased and that of MSC-320 increased within 33 h. From 33 to 48 h, the strength of MSC-320 decreases.

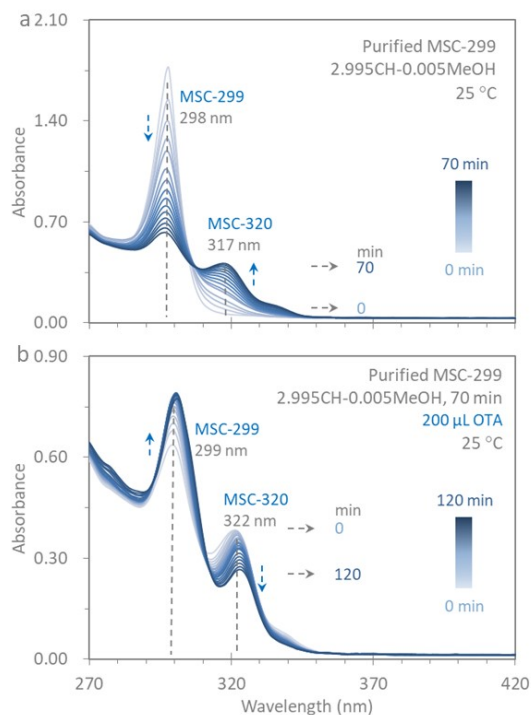


Fig. S6-2. Reversible transformation between MSC-299 and MSC-320 at room temperature studied by optical absorption spectroscopy. Purified MSC-299 was dispersed in a mixture of 2.995 mL CH and 0.005 mL MeOH.

- (a) 15 spectra were in situ collected over 70 min with an interval of 5 min. The phenomenon is similar to that of part (a) of Fig. 6.
- (b) 200 μL of OTA was added to the dispersion. 19 spectra were in situ collected over 120 min with an interval of 5 min before 60 min and of 10 min afterward. The strength of MSC-320 decreased monotonically and that of MSC-299 increased within 120 min.
- MSC-320 would transform to MSC-299 with the assistance of OTA. The transformation between MSC-299 and MSC-320 is reversible.

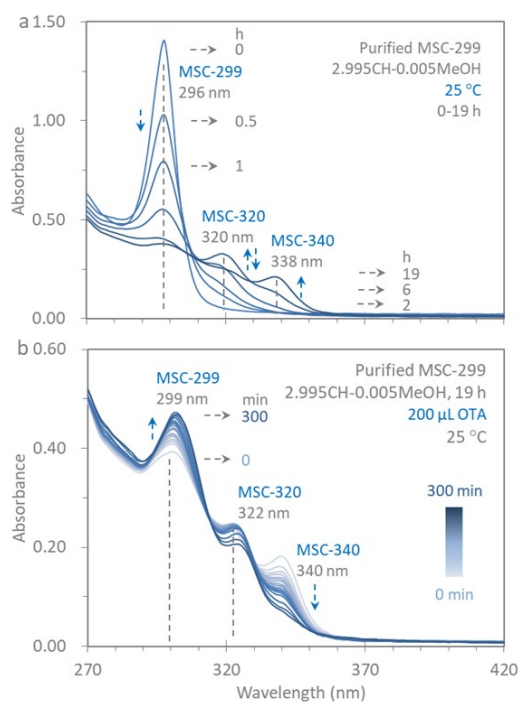


Fig. S6-3. Reversible transformation between MSC-299 and MSC-340 at room temperature studied by optical absorption spectroscopy. Purified MSC-299 was dispersed in a mixture of 2.995 mL CH and 0.005 mL MeOH.

- (a) Six spectra were collected at 0, 0.5, 1, 2, 6, 19 h, as indicated. The phenomenon is similar to that of part (a) of Fig. 6.
- (b) 200 μL of OTA was added to the dispersion. 13 spectra were in situ collected over 90 min with an interval of 5 min before 30 min and of 10 min afterward. 4 spectra were in situ collected from 120 to 300 min with an interval of 60 min. The strength of MSC-340 decreased monotonically and that of MSC-299 increased within 300 min.
- MSC-340 would transform to MSC-299 with the assistance of OTA. The transformation between MSC-299 and MSC-340 is reversible.